Journal of Optoelectronics and Advanced Materials Vol. 7, No. 1, February 2005, p. 153 - 160

Invited Paper

KINETICS OF OPTICALLY- AND THERMALLY-INDUCED DIFFUSION AND DISSOLUTION OF SILVER IN PLD $As_{40}S_{60}$ AMORPHOUS FILMS: THEIR PROPERTIES AND STRUCTURE

T. Wágner[a*], M. Krbal[a], J. Jedelský[a], Mil. Vlček [b], B. Frumarová[b], M. Frumar[a]

[a]University of Pardubice, Legion's sq. 565, 53210 Pardubice, Czech Republic
[b]Joint laboratory of Solid State Chemistry of Institute of Macromolecular Chemistry ASCR and University of Pardubice, Studentská 94, 53210 Pardubice, Czech Republic

$As_{40}S_{60}$ amorphous films were prepared by a pulsed laser deposition technique. A silver film was deposited on top of the $As_{40}S_{60}$ by vacuum thermal evaporation. Films with known silver concentrations were prepared by step-by-step optically- and thermally-induced diffusion and dissolution. The range of silver concentration was 1 – 23 at.%. The kinetics of the optically- and thermally-induced diffusion and dissolution of silver in these films was measured by optically monitoring the change in thickness of the undoped chalcogenide during broadband illumination. The compositions and a microanalysis of the reaction products were determined by electron scanning microscopy and energy-dispersive X-ray microanalysis. Optical and Raman spectroscopies were used to establish the optical properties and structures of the films.

(Received December 9, 2004; accepted January 26, 2005)

Keywords: Chalcogenide glass, PLD, OIDD, Optical properties, Structure

1. Introduction

The optically- and thermally-induced diffusion and dissolution (OIDD) of metals and amorphous chalcogenides has been widely studied e.g. [1-5]. The OIDD of metals in pulsed laser deposition (PLD) films is not fully understood, and potential applications are expected in optical and micro-optical elements such as gratings [6] and optical recording media [7]. The technique of step-by-step optically-induced dissolution and diffusion of Ag into $As_{33}S_{67}$ amorphous films prepared by thermal evaporation allowed the design of films with exact silver concentrations and thicknesses [5]. The OIDD process for silver also has potential for PLD films with similar compositions. PLD amorphous films of composition $As_{40}S_{60}$ are favorable in combination with the OIDD of silver, because this could yield optically homogeneous films with a broad range of silver content, as in thermally evaporated films [8]. Our aim was to prepare suitable silver-doped amorphous films, and to study their optical properties and structures. Knowledge of the Ag-As-S PLD films is important for potential applications. For example, it is essential to predict the performance of diffractive optical elements or fast optical switches made using these films. They could also be important in finding a suitable wavelength of light for optical recording. Also, they could yield structural information on photo-doped materials. The OIDD of Ag in PLD chalcogenide films has not been studied before, as far as we know.

2. Experimental techniques

The pulsed laser deposition system consisted of a vacuum chamber and a near-UV laser. A KrF excimer laser (Lambda Physik COMPex 102), operating at 248 nm with a constant output

*Corresponding authorl: tomas.wagner@upce.cz

energy of 290 mJ/pulse, a pulse duration of 30 ns and a repetition rate of 20 Hz was used. The energy density of the laser beam on the target was 1 $J.cm^{-2}$. The laser beam hit a bulk chalcogenide glass target at an angle of 45°. The target and substrate rotated, and their distance from each other was about 5 cm.

Thin PLD films were deposited on silica glass substrates from bulk plane-parallel samples with composition of $As_{33}S_{67}$. Bulk chalcogenide glass of composition $As_{33}S_{67}$ was prepared from the constituent pure elements. Arsenic and sulphur of 5N purity were weighed and placed in pre-cleaned and outgassed (by heating under vacuum to 900 °C) quartz ampoules. The ampoules were evacuated to a pressure of 1×10^{-3} Pa for 30 minutes, and then sealed. The synthesis was performed in a rocking furnace, with ampoules exposed to a temperature of 650 °C for 24 hours. The PLD films were prepared, with composition of $As_{40}S_{60}$. Their thickness was about 1200 nm, which is an appropriate value for the accurate evaluation of the optical parameters.

Subsequently, approximately 10 nm thick films of silver were consecutively vacuum deposited on the surface, for dissolution studies. For measurements of the kinetics, a single 100 nm thick silver film was used.

The host $As_{40}S_{60}$ films were photo-doped by the consecutive dissolution of the above thin layers of silver, resulted in homogeneous films of very good optical quality. Nine different compositions of $Ag_x(As_{0.4}S_{0.6})_{100-x}$ films were prepared. The OIDD process was carried out by illumination using a lamp house equipped with a large Fresnel lens, an IR-cutoff filter and a 500 W tungsten lamp, in the case of the step-by-step OIDD of silver. The kinetics of the optically- and thermally-induced diffusion and dissolution of silver in $As_{40}S_{60}$ amorphous films prepared by PLD was measured by optically monitoring the change in thickness of the undoped chalcogenide film during broadband illumination with the tungsten lamp ($I = 90$ mW/cm^2).

Microanalysis of the samples was performed using a JEOL JSM-5500LV electron scanning microscope and an IXRF Systems energy-dispersive X-ray microanalyser (GRESHAM Sirius 10 detector, accelerating voltage of the primary electron beam 20 kV).

The optical transmission spectra of the films were recorded using a Jasco V-570 UV/VIS/NIR spectrophotometer. In order to calculate the thickness, *d*, the refractive index, *n*, and the absorption coefficient, α, from the thin film transmission spectra, the method described by Swanepoel [9] was used. The maximum possible errors were ± 0.005 for *n*, and ± 5 nm for *d*. The optical gap, $E_{g,\,opt}$, was determined from the intercept on the energy axis of a linear fit of the high-energy data, in a plot of $(\alpha\hbar\omega)^{1/2}$ versus $\hbar\omega$, which is a widely accepted procedure (a Tauc extrapolation [10]). The optical transmission data were also analyzed on the basis of the single-effective-oscillator model proposed by Wemple and DiDomenico [11]. These authors found that the dispersion data could be described to good approximation as:

$$n^2(\omega) - 1 = E_0E_d/(E_0^2 - (\hbar\omega)^2) \quad (1)$$

where $\hbar\omega$ is the proton energy, E_0 is the oscillator energy and E_d is the oscillator strength or dispersion energy. Plotting $(n^2\text{-}1)^{-1}$ against $(\hbar\omega)^2$ allows one to determine the oscillator parameters E_0 and E_d, by fitting a straight line to the points:

$$1/n^2 - 1 = -(1 / E_d \,.\, E_0).(\hbar\omega)^2 + E_0 / E_d \quad (2)$$

The energies used were up to the proximity of the band edge, where such a linear fit is valid. The Wemple and Di Domenico expression (1) could also be useful for estimating non-linear effects in chalcogenide glasses from the linear optical index of refraction, *n*. According to Frumar [12] the Miller rule is very convenient for visible and near-infrared frequencies, which equalize the third order non-linear polarizability parameter, $\chi^{(3)}$, the so-called non-linear optical susceptibility, and the linear optical susceptibility, $\chi^{(1)}$, through the equation:

$$\chi^{(3)} = A(\chi^{(1)})^4 = A\,[E_0E_d/4\pi\,(E_0^2 - (\hbar\omega)^2)]^4 = A/(4\pi)^4\,(n_0^2 - 1)^4 \quad (3)$$

where $A = 1.7 \times 10^{-10}$ (for $\chi^{(3)}$ in esu). The covalency and ionicity of the chemical bonds strongly influence the magnitude of the non-linearity.

To a reasonable approximation, the linear index of refraction is connected to the non-linear one by $\chi^{(3)}$ [13]:

$$n_2 = 12\pi\chi^{(3)}/n_0 \tag{4}$$

Raman spectroscopy was carried out in the $As_{40}S_{60}$ films, as silver was photo-doped into the host matrix. The study was performed using a Fourier Transform (FT) Raman spectrometer (Bruker, model IFS/FRA 106). The Raman spectra were excited using a laser beam with λ = 1064 nm, having an output power of 50 mW. The wavelength of the laser beam was critical for avoiding any photostructural changes in these chalcogenide glasses, within a timescale of 100 scans. The resolution of the Raman spectrometer was 1 cm^{-1}. The PLD films ($As_{40}S_{60}$) and photodoped PLD films $Ag_x(As_{0.4}S_{0.6})_{100-x}$ were both mechanically peeled from the substrates, and immediately pressed into aluminum targets for the Raman measurements.

3. Results

The OIDD kinetic curves of silver in $As_{40}S_{60}$ PLD films, for different temperatures and illumination intensities, are shown in Figs. 1 and 2. The OIDD rate increased with increasing temperature and illumination intensity. It was found that the measured kinetic curves (i.e., doped layer thickness vs. exposure time) had complex characters. The experimental data were fitted using a composite function. As shown in Figs. 1 and 2, it consisted of a single exponential and steady state terms, as described previously [14]. A two-stage exponential/linear model: $f(t) = -a.\exp(-bt) + ct + d$, where b and c are the rate coefficients and a and d are constants, was applied. The kinetics curve shows that there are two stages to the OIDD. The first was characterized by a rate coefficient (e.g. at T = 120 °C) $k_{(exp)} = 3.02 \times 10^{-2} s^{-1}$ and the second by $k_{(lin)} = 6.43 \times 10^{-3}\ s^{-1}$, where $k_{(exp)} > k_{(lin)}$. The OIDD rates increased with increasing temperature at a constant illumination intensity (I = 90 mW/cm^2) (Fig. 1), and with increasing intensity of illumination at a constant temperature (120 °C) (Fig. 2). The OIDD activation energies were calculated according to an Arrhenius formula: $\ln(k) = -E_a/RT + \ln(K)$ or $\ln(k) = -Ea/RI + \ln(K)$, where T is the temperature [K] and I is the light intensity [mW/cm^2] (Figs. 3 and 4). The OIDD activation energy values were obtained from the temperature dependence kinetics: $E_{a(exp),T}$ = 12.8 kJ/mol, $E_{a(lin),T}$ = 33.4 kJ/mol, and from the light intensity dependence kinetics: $E_{a(exp),I}$ = 1.14 kJ/mol, $E_{a(lin),I}$ = 1.19 kJ/mol.

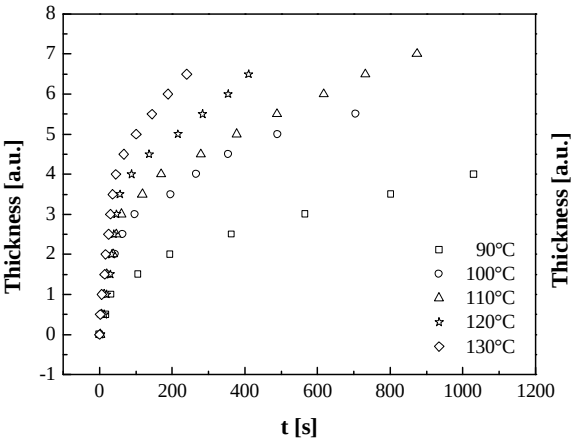

Fig. 1. Kinetics of the OIDD of Ag into PLD $As_{40}S_{60}$ films, measured at different temperatures for a constant illumination intensity.

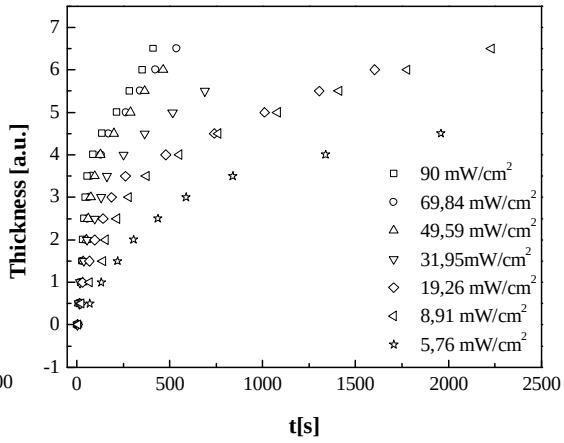

Fig. 2. Kinetics of the OIDD of Ag into PLD $As_{40}S_{60}$ films, measured at different illumination intensities for a constant temperature.

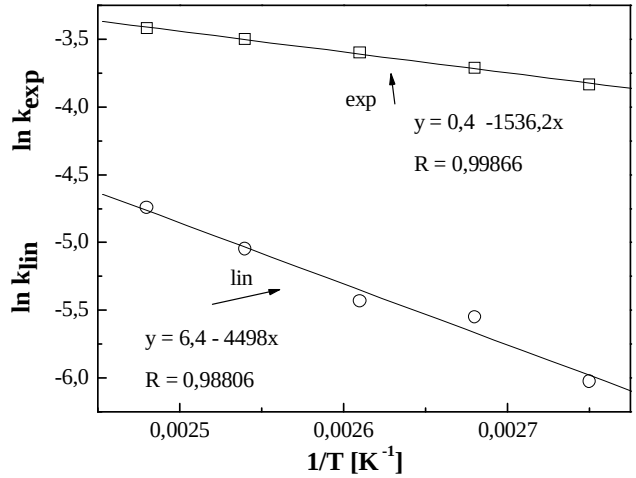

Fig. 3. The Arrhenius-type dependences of ln(k) = f (T) allow the calculation of activation energies ($E_{a(exp),I}$ and $E_{a(lin),I}$) of OIDD Ag into PLD $As_{40}S_{60}$ at a constant illumination intensity of I = 0.09 Wcm^{-2}, at different temperatures.

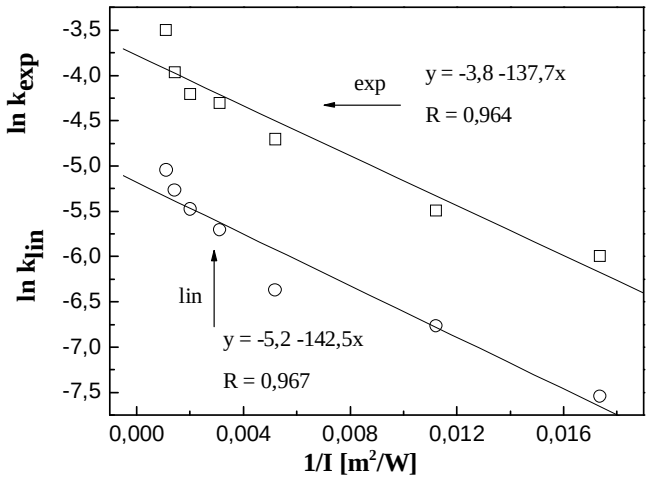

Fig. 4. The Arrhenius type dependences of ln(k) = f (I) allow the calculation of activation energies ($E_{a(exp),I}$ and $E_{a(lin),I}$) of OIDD Ag into PLD $As_{40}S_{60}$ at a constant temperature of 120 °C, at different illumination intensities.

The PLD technique followed by the OIDD of silver allowed the preparation of a set of nine different samples of $Ag_x(As_{0.4}S_{0.6})_{100-x}$ films, where x ranged from 0 to 23 at.%. The compositions were confirmed by EDX analysis. Using the approach due to Kosa [8], the homogeneity of the doped films was clearly confirmed by the corresponding spectral dependence of the transmission, where no shrinkage of the interference fringes was observed, as is clear from Fig. 1. With increasing silver content, the modulation depth of the interference fringes increased, indicating that in the each case we measured a "new material". Fig. 5 demonstrates an also almost linear dependence of the red shift on the silver content. Silver dissolution also changed other thin film characteristics, e.g. the optical band gap, $E_{g,opt}$, and the film thickness, d, both increased linearly with increasing silver content in the films. These conclusions are drawn from Fig. 6. The dependence of the single-oscillator parameters, E_0 and E_d, on the silver content is shown in Fig. 7.

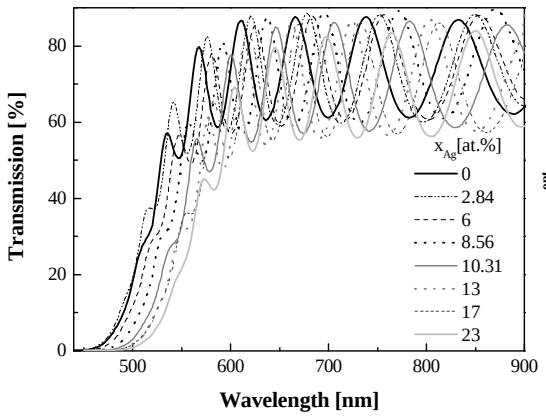

Fig. 5. Transmission spectra of $Ag_x(As_{0.4}S_{0.6})_{100-x}$ films prepared by the OIDD of silver into PLD $As_{40}S_{60}$ amorphous films.

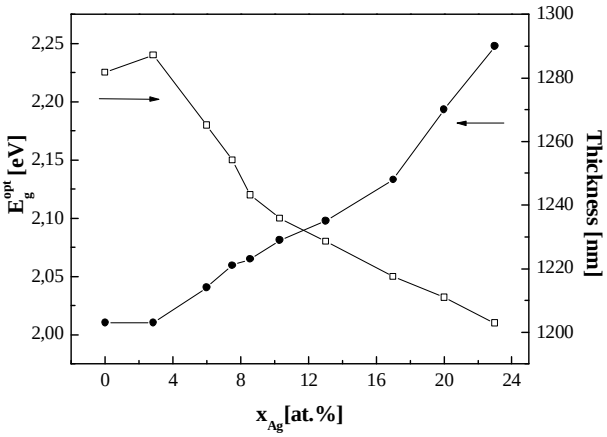

Fig. 6. Optical gap and film thickness versus silver content in the $Ag_x(As_{0.4}S_{0.6})_{100-x}$ films. The lines are guides to the eye.

The index of refraction of PLD $As_{40}S_{60}$ films was increased significantly by the OIDD of silver (Fig. 8). Also, calculations of the non-linear index of refraction, n_2, according to Eq. (4), showed an increasing value with the concentration of silver introduced into the PLD films (Fig. 9).

The Raman spectra measured in the Ag-As-S films are shown in Fig. 8. The spectra were interpreted using the approach described in [15]. The illuminated $As_{40}S_{60}$ film (Fig. 10, $x_{Ag} = 0$) contained strong bands at 340 ($AsS_{2/3}$ units) and 358 cm^{-1} (As_4S_4 units), The subsequent step-by-step OIDD process of silver in $As_{40}S_{60}$ films led to the appearance of new strong bands at 376 cm^{-1} (AsS_3 pyramids or As_3S_6 units [16] connected by S-Ag-S linkage or AgS_3 pyramids [17]) and at 272 cm^{-1} (As_4S_4-pararealgar units [18]). The decrease of the intensities of the main bands characteristic of the $As_{40}S_{60}$ film, and the formation of new bands due to the silver content in $Ag_x(As_{0.4}S_{0.6})_{100-x}$, is shown in Fig. 10.

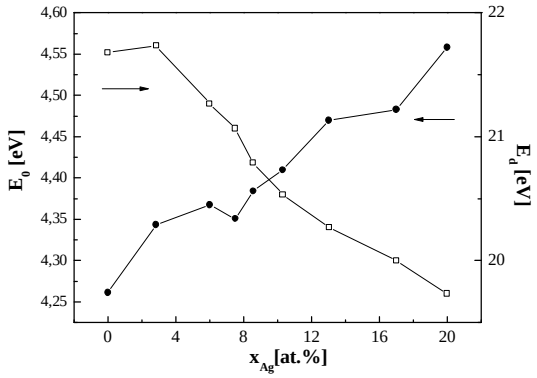

Fig. 7. Silver content dependence of the single-effective - oscillator parameters E_0 a nd E_d. The lines are guides to the eye.

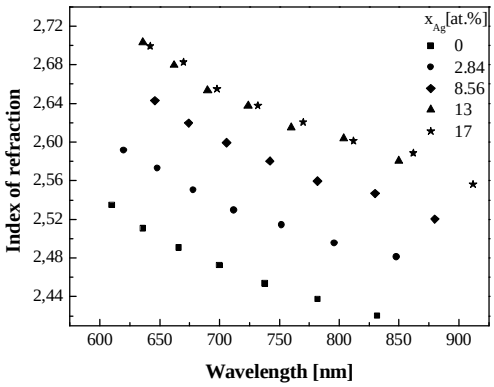

Fig. 8. Linear refractive indices as a function of the silver content in $Ag_x(As_{0.4}S_{0.6})_{100-x}$ films prepared by OIDD.

4. Discussion

The kinetic data obtained are characterized by two rate coefficients, implying that the OIDD phenomenon involves two different consecutive processes. It is suggested that in stage 1 (the exponential stage) an Ag-doped layer is formed. It is further suggested that at the beginning of the

exponential stage of OIDD, when the Ag-doped layer is formed and is sufficiently thin, the process can be influenced by electrical space charges, resulting from the presence of a contact potential on the metal/p-type semiconductor boundary, which is the case for the $Ag/As_{40}S_{60}$ bilayer system [16]. Stage 2 (linear) is typical of a chemical process, in which the driving force is a chemical reaction on the boundary (the silver doped/undoped part of the chalcogenide) [16, 17].

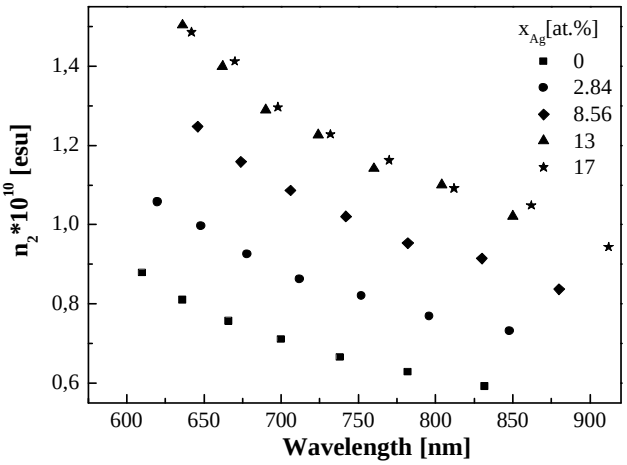

Fig. 9. Non-linear refractive indeces in dependence on silver content in $Ag_x(As_{0.4}S_{0.6})_{100-x}$ films prepared by OIDD.

The activation energies were $E_{a(exp),T}$ = 12.8 kJ/mol, $E_{a(lin),T}$ = 33.4 kJ/mol, $E_{a(exp),I}$ = 1.14 kJ/mol and $E_{a(lin),I}$ = 1.19 kJ/mol. The existence of two activation energies, i.e. $E_{a(lin),T}$ and $E_{a(lin),I}$, could be explained with the help of the Anderson-Stewart model [19] (Fig. 11). It could be generally concluded that the thermally activated process is connected with amorphous network vibrations, and that the optically activated process can be related to the optically-induced breaking of Ag–S, As–S and S–S bonds, causing the formation of electron-hole pairs.

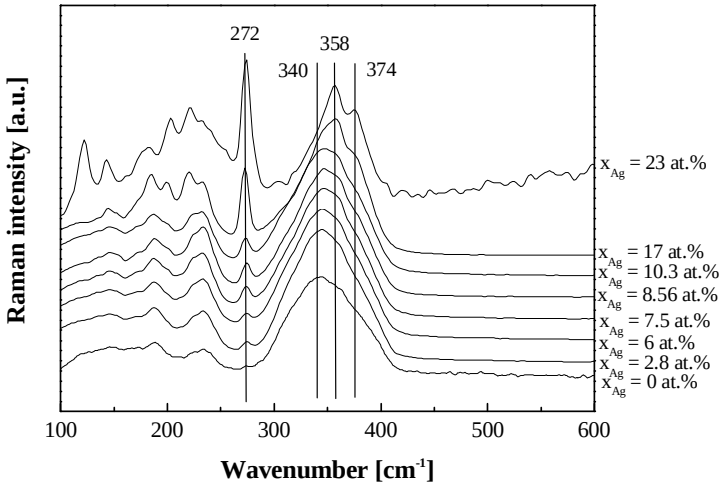

Fig. 10. Raman spectra of $Ag_x(As_{0.4}S_{0.6})_{100-x}$ films prepared by OIDD of silver into PLD $As_{40}S_{60}$ amorphous films.

The decrease of the $E_{g,\ opt}$ value is in a good agreement with similar experiments on thermally evaporated films [8]. The decrease of the $E_{g,\ opt}$ value with increasing silver content is explained by the fact that the Ag-S bonds have a smaller binding energy than the As-S bonds. This therefore leads to a smaller energy splitting between the valence and conduction states. The oscillator energy, E_0, is the average energy gap, and to a good approximation it varies in proportion to the optical bandgap ($C.E_0 = E_{g,\ opt}$, where $C \approx 2.1$). E_d serves as a measure of the strength of the interband transitions. An important achievement of the Wemple-DiDomenico model is that it relates the dispersion energy, E_d, to other physical parameters of materials, through an empirical formula:

$$E_d = \beta N_c Z_a N_e \text{ (eV)}, \tag{5}$$

where β is a constant with either an ionic or a covalent value ($\beta = 0.37$ eV), N_c is the coordination of the cations, Z_a is the formal valency of the anion and N_e is the effective number of valence electrons per anion. An increase in the E_d value means an increase in the average cation coordination number. The presence of silver obviously leads to an increase in the silver coordination number. This has been proved in numerous studies of evaporated films and bulk glasses with values between 3 and 4 [8, 20]. Ag–S band formation was indirectly proved by the fact that As_4S_4 structural units increase the magnitude of the band at 272 cm^{-1}. The silver bonding to the binary As-S amorphous network of PLD films is visible from the Raman spectra. The E_d value in ternary systems is, according to Kim [21], also related to the bond length, X, ($E_d \sim X^2$), explaining why the films expand during the OIDD of silver. Clearly, OIDD produces a very significant change in the linear refractive index compared to PLD $As_{40}S_{60}$ films: ~ 0.2 for the highest silver concentration. The linear index of refraction is, to a reasonable approximation, connected to the non-linear one by $\chi^{(3)}$. The polarisable atoms with lone pairs (e.g. chalcogens) influence the $\chi^{(3)}$ value. However, the presence of heavy atoms with easily polarisable electron clouds (e.g. Ag) is even more effective. The $\chi^{(3)}$ value is also increasing due to the fact that silver improves the polymerization and strength of the bonds in the amorphous network.

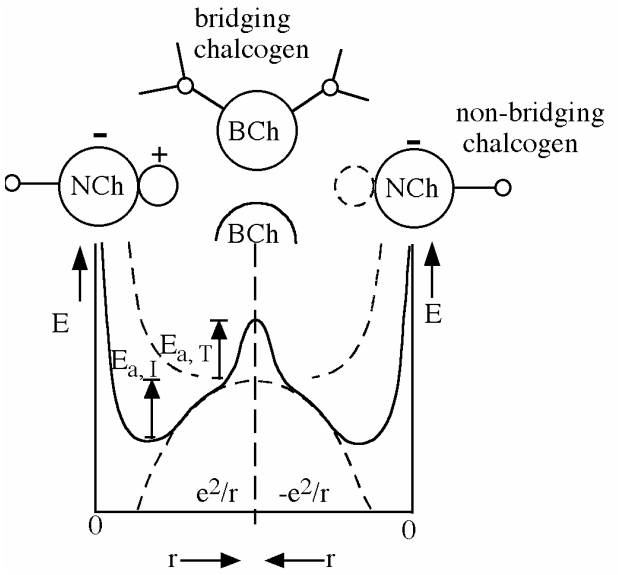

Fig. 11. Configuration–coordinate diagram proposed to account for the energetics of ionic transport in glasses [19].

5. Conclusions

Thin amorphous films with composition $Ag_x(As_{0.4}S_{0.6})_{100-x}$, where x varied from 0 to 23 at.%, were prepared by the OIDD of Ag in $As_{40}S_{60}$ PLD films. The kinetics of the OIDD of Ag in $As_{40}S_{60}$ PLD films were measured. The data showed a two-stage reaction process (with exponential

and linear regions). We measured the optical bandgap, $E_{g,opt}$, (2.24 – 2.01 eV), the film thicknesses, and the change of the refractive index of dispersion $\Delta n(\lambda) \sim 0.2$ in the $Ag_x(As_{0.4}S_{0.6})_{100-x}$ films. The samples containing silver were prepared by the process of OIDD of Ag. Dissolution of Ag into the matrix introduced new Ag-S bonds with smaller binding energies than those of the As-S bonds. This explains the decrease in the optical bandgap with increasing Ag content. Raman spectra showed an increase in the vibration of As_4S_4 structural units with increasing silver content. Analysis of the dispersion data on the basis of the Wemple-DiDomenico single-effective-oscillator model indicated that the oscillator energy E_0 varied in proportion to $E_{g,opt,,}$ with a constant of proportionality C = 2.1. The value of the oscillator strength E_d increased with increasing Ag content, since silver is highly coordinated in the matrix. The E_d value was related to the bond length. The values of n, E_0 and E_d enabled the calculation of the non-linear optical susceptibility, $\chi^{(3)}$, according to Miller's rule. The non-linear index of refraction increased with increasing Ag content, by a value of $\Delta n_2 \sim 6.10^{-11}$.

Acknowledgements

The authors welcome the support of Research Center project LN00A028 of the University of Pardubice, and grants ME 633 and FRVŠ 729 G1 of Ministry Education,Youth and Sports of Czech Republic.

References

[1] M. T. Kostyshin, E. V. Mikhailovskaya, P. F. Romanenko, Sov. Phys. Solid State **8,** 451 (1966).
[2] M. Krbal, T. Wágner, T. Kohoutek, Mir. Vlček, Mil. Vlček, M. Frumar, J. Optoelectron. Adv. Mater. **5**, 1147 (2003).
[3] A. V. Kolobov, Photo-induced metastability in amorphous semiconductors, Wiley-VCH Weinheim, 2003.
[4] Ke. Tanaka, T. Gotoh: in Andrei Andriesh Homage Book, INOE & INFM Publishing House, Bucharest, Romania (1999) p. 29.
[5] T. Wagner, G. Dale, P. J. S. Ewen, A. E. Owen, V. Perina, J. Appl. Phys. **87,** 7758 (2000).
[6] E. Hajto, P. J. S. Ewen, R. E. Belford, A. E. Owen, Thin Solid Films **200,** 229 (1991).
[7] T. Ohta, J. Optoelectron. Adv. Mater. **3,** 609 (2001).
[8] T. I. Kosa, T. Wagner, P. J. S. Ewen, A. E. Owen, Phil. Mag. B **71,** 311 (1995).
[9] R. Swanepoel, J. Phys. E.: Sci. Instrum. **16,** 1214 (1983).
[10] J. Tauc, in: Amorphous and Liquid Semiconductors, ed. J. Tauc (Plenum, New York, 1974), p. 171.
[11] S. H. Wemple, M. Di Domenico, Phys. Rev. B **3,** 3767 (1971).
[12] M. Frumar, J. Jedelsky, B. Frumarova, T. Wagner, M. Hrdlicka, J. Non-Cryst. Solids, **326-327,** 399 (2003).
[13] H. Tichá, L. Tichý, J. Optoelectron, Adv. Mater. **4,** 381 (2002).
[14] T. Wagner, M. Vlcek, V. Smrcka, P. J. S. Ewen, A. E. Owen, J. Non-Cryst. Solids 164-166, 1255 (1993).
[15] G. Lukovski, F. L. Geils, R. C. Keezer, The Structure of Non-Crystalline Materials (Taylor and Francis, London, 1977) p. 127.
[16] V. Yu. Slivka, Yu. M. Vysocanskij, V. A. Stefanovic, V. S. Gerasimenko, D. V. Cepur, Sov. Phys. Sol. Stat. **24,** 696 (1982).
[17] I. T. Penfold, P. S. Salmon, Phys. Rev. Lett. **64,** 2164 (1990).
[18] M. Muniz-Miranda, G. Sbrana, P. Bonazzi, S. Menchetti, G. Pratesi, Spectrochimica acta, part A **52,** 1391 (1996).
[19] H. Fritzsche, in Andrei Andriesh Homage Book, INOE & INFM Publishing House, Bucharest, Romania (1999) p. 53.
[20] S. H. Kim, T. Yoko, J. Am. Ceram. Soc. **78,** 1061 (1995).
[21] S. R. Elliott, Physics of Amorphous Materials, Longman Scientific Technical Essen, 1990, p. 247.